01 Apr 2009

A System Design Approach for Unattended Solar Energy Harvesting Supply

Jonathan W. Kimball
Missouri University of Science and Technology, kimballjw@mst.edu

Brian T. Kuhn

Robert S. Balog

Recommended Citation

J. W. Kimball et al., "A System Design Approach for Unattended Solar Energy Harvesting Supply," *IEEE Transactions on Power Electronics*, vol. 24, no. 4, pp. 952-962, Institute of Electrical and Electronics Engineers (IEEE), Apr 2009.
The definitive version is available at https://doi.org/10.1109/TPEL.2008.2009056

A System Design Approach for Unattended Solar Energy Harvesting Supply

Jonathan W. Kimball, *Senior Member, IEEE*, Brian T. Kuhn, *Senior Member, IEEE*, and Robert S. Balog, *Senior Member, IEEE*

***Abstract*—Remote devices, such as sensors and communications devices, require continuously available power. In many applications, conventional approaches are too expensive, too large, or unreliable. For short-term needs, primary batteries may be used. However, they do not scale up well for long-term installations. Instead, energy harvesting methods must be used. Here, a system design approach is introduced that results in a highly reliable, highly available energy harvesting device for remote applications. First, a simulation method that uses climate data and target availability produces Pareto curves for energy storage and generation. This step determines the energy storage requirement in watt-hours and the energy generation requirement in watts. Cost, size, reliability, and longevity requirements are considered to choose particular storage and generation technologies, and then to specify particular components. The overall energy processing system is designed for modularity, fault tolerance, and energy flow control capability. Maximum power point tracking is used to optimize solar panel performance. The result is a highly reliable, highly available power source. Several prototypes have been constructed and tested. Experimental results are shown for one device that uses multicrystalline silicon solar cells and lithium–iron–phosphate batteries to achieve 100% availability. Future designers can use the same approach to design systems for a wide range of power requirements and installation locations.**

***Index Terms*—Battery, energy harvesting, energy management , long life, photovoltaic, remote power, ultracapacitor, unattended operation.**

I. Introduction

MANY REMOTE unattended loads require continuously available power sources with long lifetimes. Examples of such loads include agricultural sensors and controls, geological and meteorological sensors, broadband Internet hardware, and surveillance equipment. While the average power requirements of these loads are generally low, the accumulated lifetime energy requirement may be large. This paper details a design approach that can be used for an energy harvesting system to minimize the cost and size of the power source. The new methodology is appropriate for systems that cannot be serviced after installation, due to location or labor costs.

Manuscript received July 31, 2008; revised October 23, 2008. First published nulldate; current version published nulldate. Recommended for publication by Associate Editor K. Ngo.

J. W. Kimball is with Missouri University of Science and Technology, Rolla, MO 65409 USA (e-mail: kimballjw@mst.edu).

B. T. Kuhn and R. S. Balog are with SmartSpark Energy Systems, Inc., Champaign, IL 61820 USA (e-mail: b.kuhn@smartsparkenergy.com; r.balog@smartsparkenergy.com).

Color versions of one or more of the figures in this paper are available online at http://ieeexplore.ieee.org.

Digital Object Identifier 10.1109/TPEL.2008.2009056

A system topology that integrates the solar generation, energy storage, and control process will be discussed. An important design tradeoff is energy storage versus solar panel size for a given availability. The solar panel supplies energy through a power electronic converter during the day to support the load; excess energy is stored. At night or when there is not enough solar energy to support the load, power is withdrawn from the energy storage. Analytical and numerical models of the system were developed to allow computer simulations of a variety of solar insolation, load, availability, and geographical location scenarios. Historical solar insolation data from the National Solar Radiation Database (NSRDB) was used as the input to approximate realistic environmental conditions for a variety of U.S. locations [1]. The model was then used as a design tool for specification of the size and rating of the solar panels and storage. Hardware prototypes were constructed and deployed in Champaign, IL. Monitoring and data collection confirmed that the design worked as anticipated.

The system described in this paper falls into the broad category of energy harvesting. Various energy sources have been proposed for such systems, such as mechanical vibration [2]–[5], ambient radio frequency energy [6], [7], wind [8]–[11], and solar energy [12]–[14]. Each has benefits and drawbacks. Solar energy has the most benefits and the least drawbacks, compared to other technologies and is the technology chosen for the system described in this paper. As noted in [13], solar energy has the greatest power density for these applications. Other sources can also be included using similar design principles.

Conventional power sources for remote loads are all lacking in some respect. Primary batteries are attractive options for a device with a very low energy requirement or limited lifetime, but do not scale well for many applications. Connection to the ac mains may be expensive or unavailable in the desired installation location. Many energy harvesting systems are oversized, either because there is no controller to manage and optimize the energy flow or because they are designed for worst-case scenarios. The approach described in this paper includes sophisticated energy management and device sizing to achieve a small, low-cost system with high availability. *Availability* is a measure of the fraction of time that energy is available for the load, as detailed in Section III.

The goals of this paper are to introduce a new sizing method based on availability and identify key considerations for component and topology selections. The proposed energy harvesting device differs substantially from existing devices; so different considerations apply. For example, the device

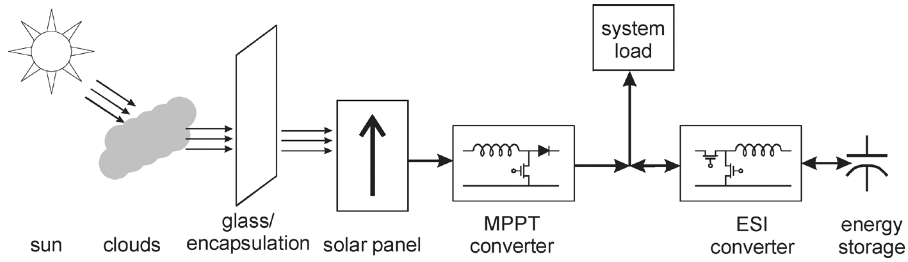

Fig. 1. System design—energy flow diagram.

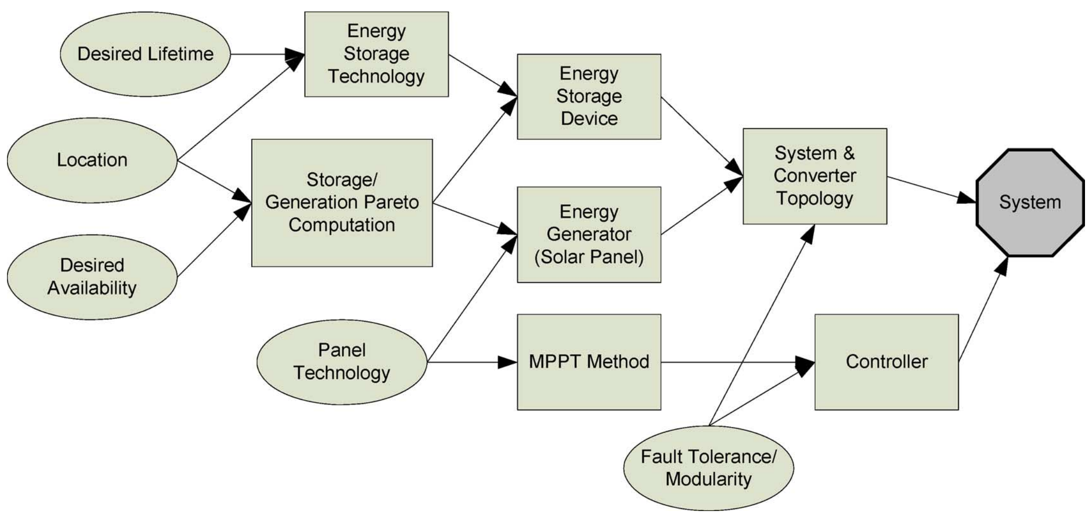

Fig. 2. Design flow influence diagram.

typically cannot be serviced; so recovery from faults must be entirely self-contained, as discussed in Section VII. Maximum power point tracking (MPPT) methods, discussed in Section V, should focus on performance at low insolation levels, rather than on maximum energy production at high insolation levels. Throughout the paper, such differences are identified.

The following sections detail the design methodology. Section II discusses the overall system considerations and design flow. Section III details a method of computing the required energy storage and energy generation based on data from the NSRDB, the load profile, and the desired availability. Section IV identifies appropriate energy storage technologies, and concludes that lithium-ion batteries and ultracapacitors are the best choices for the application. Section V identifies two MPPT methods that have low control complexity and acceptable performance at low insolation levels. Sections VI and VII discuss modularity and fault tolerance.

Experimental results are presented in Section VIII. Several systems have been designed for 100% availability in Champaign, IL, for different load profiles. Performance data indicate that the systems perform as expected and are able to deliver power continuously despite low insolation levels.

II. System Energy Circuit

The energy flow block diagram for an example system that integrates solar generation, energy storage, and control processes is shown in Fig. 1 [15]. This system draws energy from the sun, which is then processed to produce regulated dc voltage for the system load. The input converter is configured as an MPPT converter [16], which ensures that the maximum available solar energy is harnessed from the solar panel, allowing the required size of the panel to be minimized. The energy storage interface (ESI) converter is a bidirectional power electronic circuit that stores excess energy gathered during daylight hours and delivers it to the load at night or on days without sufficient solar energy to support the load [17]. The ESI converter also manages the energy storage device to ensure long life and protects the system against faults.

Fig. 2 shows the overall design flow. Inputs, shown as ovals, include the desired system lifetime, the desired availability, the location where the device will be installed, the photovoltaic panel technology, and any requirements for fault tolerance or modularity. The location and desired availability determine how much energy storage and energy generation are required. Whereas a worst-case approach would consider the two aspects separately, the climatic simulation method shown in Section III considers the interaction between storage and generation. The output of the simulation is a curve that relates storage (in watt-hours) and generation capacity (in watts). Given the desired lifetime in a particular location, which determines the ambient temperature, an energy storage technology can be chosen, as discussed in Section IV. Typical choices are lithium-ion variants and ultracapacitors, depending on the size and longevity requirements. A specific combination of an energy storage device and a solar panel can be chosen from the Pareto curve based on cost, size, or other factors. The electronics—the power converter topology, the system-level topology, MPPT, and other controls—are then designed around the chosen energy storage and generation devices to complete the system.

The topology in Fig. 1 is representative of the main functions that should be included in a remote, unattended power source. Other system topologies, such as [14], can achieve most of the same functions but with different efficiency tradeoffs. Multiport converter topologies, such as [18]– [20], are also feasible as long as appropriate controllers are in place. In particular, topologies such as [18] and [20], which are transformer-isolated, may be useful where either a large voltage gain or galvanic isolation is needed for the sensor. An important advantage of the topology in Fig. 1 is that the energy generation, energy storage, and load are all decoupled through separate switching power converters. Any remote power source should include the following functions:

1) an energy source;
2) power generation maximization (MPPT);
3) energy flow monitoring and management;
4) energy storage device conditioning for long life;
5) output voltage regulation;
6) fault protection;
7) fault tolerance.

Fault tolerance is critical for an unattended power source. If a fault should occur that causes the system to fail, even on a transient basis, there is no means for intervention to "reset" the system. Faults to consider include failed or degraded components, short circuits, or overloads on the output, and erroneous software operation. So, power converter topologies, system topologies, and control methods should include self-recovery modes and mechanisms, as detailed in Section VII. One-time devices, such as fuses, should be eschewed in favor of resettable devices.

The control circuitry, not shown in Fig. 1, is responsible for achieving these various functions. There are many methods in the literature for each function; for example, MPPT methods resulted in more than 90 papers prior to 2005 [21], and many more since then. Subsequent sections will identify some of the important considerations for selecting a particular energy flow control algorithm. An overriding objective that applies throughout, though, is to minimize quiescent power consumption. When comparing two methods, the extra power consumption of a superior method must be counted against that method. Consider two MPPT methods, "A" and "B," with different tracking accuracies, 90% and 95%, respectively. If method B requires circuitry that consumes an extra 10 mW, then method A will be favored unless the average power generation exceeds 200 mW. Similar principles apply to all subsystems, e.g., more effective energy management circuits that consume more power may not provide a net advantage.

In a solar energy harvesting system, there are many mechanisms that contribute to the overall conversion efficiency. The foremost condition is the location in which the system is deployed. Latitude as well as the typical weather patterns at the deployment location play a large role in determining the amount of sunlight reaching the energy harvesting system, and hence affect the overall performance of the system. The solar panel technology further limits power generation. Multicrystalline silicon cells rarely exceed 15% insolation-to-electricity efficiency. Advanced multiple-junction cell efficiencies can reach or exceed 30% but cost orders-of-magnitude more and are rarely used in terrestrial applications [22]. Other efficiency loss mechanisms include the optical loss of the glass encapsulation, electrical losses in both converters, and storage losses. A key design goal is to minimize losses in the power electronics components.

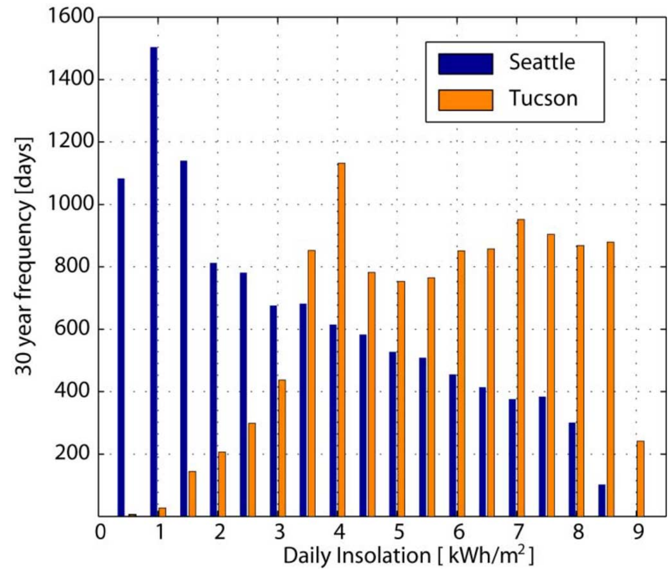

Fig. 3. Thirty-year histogram of daily insolation.

III. Availability Model

A. Methodology

Historical solar insolation data, available from the NSRDB for 239 sites in the United States over a 30-year period, from 1961 to 1990, have been used to approximate realistic environmental conditions for a variety of locations [1]. Two locations that represent a range of climate, weather, and insolation patterns are Seattle, WA, and Tucson, AZ. The histogram of the 30-year insolation data, shown in Fig. 3, reveals that Seattle has a high number of days with low solar insolation resulting from the combined effects of higher latitude and relatively heavy cloud cover during winter months. Over the 30 years of data in Seattle, the best day had an incident energy density of 8684 Wh/m^2 and the worst day had only 156 Wh/m^2. Conversely, Tucson has only a low number of days with low insolation—a best day of 13 626 Wh/m^2 and a worst day of 990 Wh/m^2. Thus, Seattle and Tucson can be considered as extreme environments for design comparisons. In an actual design, the city nearest to the actual installation should be chosen for all computations.

Using the hourly incident solar illumination from the NSRDB, a model was constructed to predict the overall availability of a given system over the entire dataset. The algorithm, shown in pseudocode in Fig. 4, computes the number of hours when the stored energy falls to zero, and hence, the system is unable to provide energy to the load. This number of hours is converted to an overall availability of the system over the dataset period.

```
//initialize model
I = 0          //increment over hourly datapoints in dataset
BAD_HOURS = 0  //count number of bad hours detected
STORED_ENERGY = MAX_AVAIL_STORED   //begin full

//loop over all hours in dataset
WHILE (NOT end_of_dataset)
   I = I + 1
   INPUT_ENERGY = SOLAR_ENERGY(I) - (panel_and_MPPT_losses)
   NET_ENERGY = INPUT_ENERGY - LOAD_ENERGY(I) //can be + or -
   STORED_ENERGY = STORED_ENERGY + NET_ENERGY - (battery_and_ESI_losses)
   IF (STORED_ENERGY > MAX_AVAIL_STORED)
      STORED_ENERGY = MAX_AVAIL_STORED //throw away excess since full
   END IF
   IF (STORED_ENERGY < 0)        //no stored energy remaining
      STORED_ENERGY = 0          //don't allow stored energy to go negative
      BAD_HOURS = BAD_HOURS + 1 //count the bad hours
   END IF
END WHILE

//compute availability
AVAILABILITY = 1 - BAD_HOURS/I  //compute overall availability over the dataset
```

Fig. 4. Pseudocode for availability determination.

TABLE I
TEN-YEAR UNAVAILABILITY

Availability	*Unavailability*
99.999%	53 minutes
99.99%	8.8 hours
99.9%	3.7 days
99%	37 days
90%	52 weeks

Availability, the fraction of the time when energy is available, is a key figure of merit for the proposed system. It is important to make a clear distinction between availability and reliability. Reliability is the ability of the system to operate without failure; availability is the ability of the system to supply power to the load. A highly reliable photovoltaic energy system, where the components are not prone to failure, can have low availability if there is insufficient energy storage to support the load's power requirements during the night or during an overcast day, or if there is insufficient energy generation to recharge the system. Table I gives examples of system availability and the resulting unavailability over a ten-year period—the target operating life for the design in this paper.

The model of the system in Fig. 1 was used in conjunction with the 30-year hourly solar data [1] for Tucson and Seattle to determine the size of the PV panel and amount of storage required to achieve a desired availability. The results, shown in Fig. 5, assume a load of 50 Wh per day (continuous load evenly distributed through the day). For these studies, the panel size is specified in peak watts, the way the panel is specified from the manufacturer-given industry standard test conditions (1000 W/m ^{2}, 25 °C, AM1.5 [23]). The peak watt output can map into various physical sizes, depending on the PV technology. Energy storage is specified in watt-hours. The nature of the energy storage, which will be discussed in Section IV, similarly determines the mapping from watt-hours into physical size. Initially, losses in the power converters can be neglected, as they are here, to give a best possible case scenario. As they become known, or at least bounded, the studies can be repeated to improve the accuracy of the availability prediction.

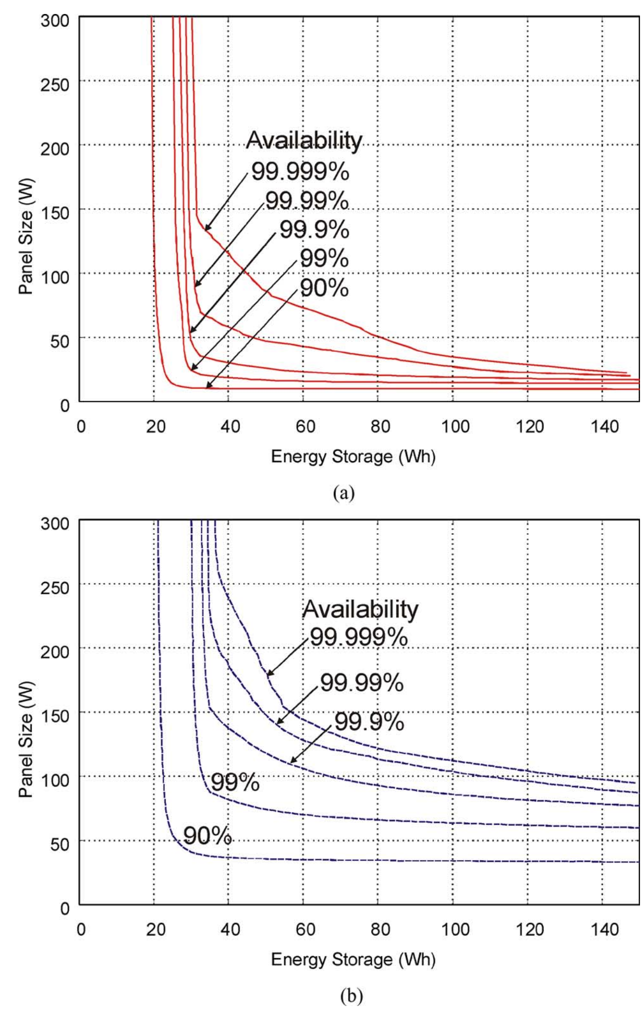

Fig. 5. Effect of geography on solar panel size, energy storage requirement, and system availability. (a) Tucson. (b) Seattle.

A design based on the historical data does not guarantee worst-case system availability; rather, it represents one reasonable engineering solution. A worst-case design, specifying

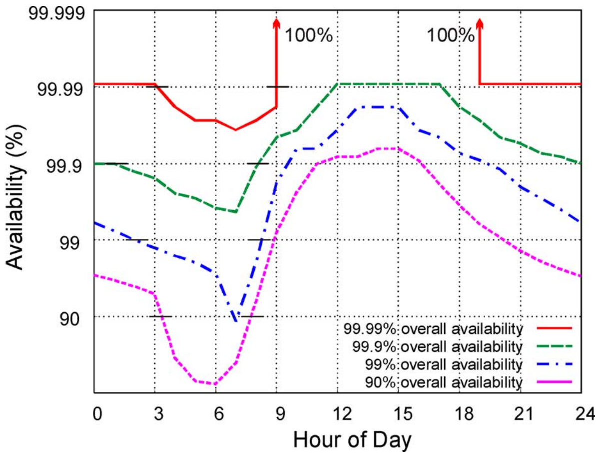

Fig. 6. Predicted availability versus time of day in Tucson.

TABLE II
SIZING FOR CURVES ON FIG. 6

System	*Availability*	*Panel*	*Storage*
1	99.99%	70 W	32.5 Wh
2	99.9%	35 W	33.3 Wh
3	99%	25 W	29.9 Wh
4	90%	17 W	24.0 Wh

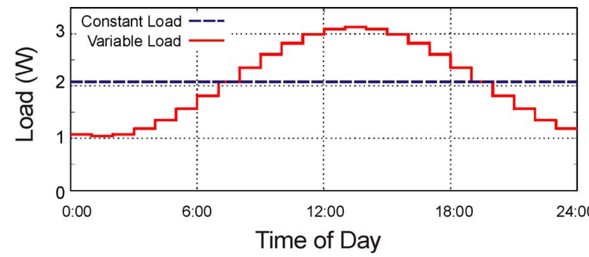

Fig. 7. Example of two 50 Wh per day load profiles.

absolute limits on availability (two days without solar insolation, for example), could be considered, but would result in a larger and more expensive system.

B. Energy Storage Versus Energy Generation

A specified level of availability can be achieved with many configurations of a system. In Tucson, for example, 99.99% availability can be reached via a continuum of panel/energy storage sizes, as illustrated in Fig. 5. At the extrema, a panel of at least 20 W must be used with very large energy storage, or at least 28.5 Wh of energy storage must be used with a very large panel, to achieve availability of 99.99%. Another solution for this system would use a 71-W solar panel with 33 Wh of energy storage. Since system cost increases with the size of the PV panel and energy storage, the design can be optimized to yield the lowest cost design for a specified availability at a particular geographical location. The optimization must consider a wide range of variables, both technical (such as PV and energy storage device characteristics) and nontechnical (such as supply chains and logistics). PV panels with various different cell technologies may be custom-built, but are more readily available in fixed increments. Energy storage devices are available in fixed increments; however, the charge management scheme and degradation over the lifetime of the unit may cause the actual energy storage capability to vary from "rated" capacity. Projected area, volume, and mass may be limited by the deployment site or method. Since PV panels are sized for area and energy storage devices are sized for volume or mass, size constraints may favor one or the other.

In addition to the availability of the system over the entire operating period, it is interesting to look at the predicted availability of the system as a function of time throughout the day. Since the sun shines during the daytime, daytime hours have a higher availability than the dark hours just before sunrise. Fig. 6 shows the predicted availability of four systems in Tucson with their availability plotted by hour of the day. The systems were chosen such that the overall availability of the systems was 99.99%, 99.9%, 99%, and 90%. The solar panel sizes and energy storage for these systems are given in Table II . The panel ratings and storage capacities are representative points near corners in the Pareto chart [Fig. 5(a)] and were chosen to show trends. Other choices would have availability versus time graphs that resemble Fig. 6, but differ slightly in details. We see that these systems operate above their overall specified availability for most of the day, except during the early morning hours. In many applications, the availability requirement may not be uniform throughout the day. In the case of a communications system, such as for wireless access to rural locations, reduced system availability may be tolerated during off-peak hours such as early morning. This is an important design consideration that can substantially lower the overall system cost.

Another factor that can influence the performance of the system is the scheduling of the load, also called the load profile, throughout the day. So far, the models have assumed that the load is constant or, equivalently, a pulsed load uniformly distributed throughout each hour of every day. In many applications, such as rural broadband, the load may peak during the daytime hours when more people are using the system. Fig. 7 shows a load profile that peaks at 2 P.M. in the afternoon. A system with this load profile has less demand during the night hours when the system power is supplied exclusively from the stored energy. This translates into reduced requirements for the amount of energy stored in the system to meet a given availability target, as shown in Fig. 8. Other load profiles will also alter the tradeoff curves. For example, a lighting application, for which the load peaks at night, requires greater energy storage than an application with constant load.

IV. ENERGY STORAGE TECHNOLOGIES

There are many energy storage technologies, each of which may offer advantages for a particular application. In this application, the relative power levels are low, but a high availability requirement coupled with a long lifetime quickly narrows the applicable technologies. Energy density and operating temperature range are key design considerations when selecting the most appropriate storage technology. There are a number of energy storage technologies that have been considered for advanced power applications [24]. However, only batteries and ultracapacitors meet the requirements of long, unattended service life. Superconducting magnetic energy storage devices require cryogenic systems, flywheel systems have high self-discharge, and

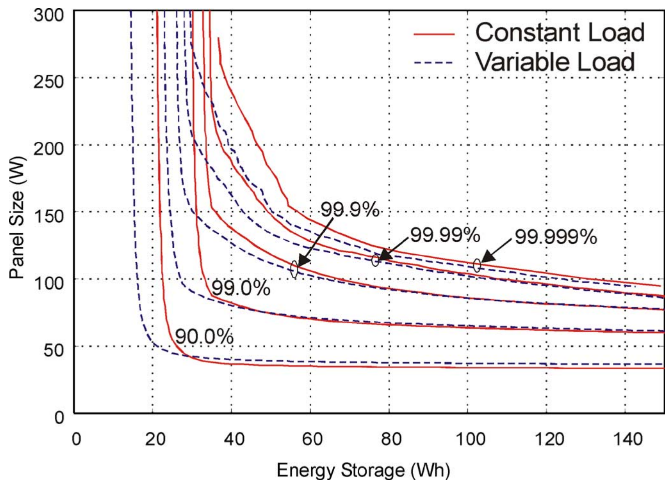

Fig. 8. Constant load versus variable load in Seattle.

technologies such as compressed air are not yet mature. Ultracapacitors are most well known for having high power density, but they also have excellent lifetime qualities that make them superior to batteries when the energy requirements are lower, and reliability is of paramount importance. Batteries are applicable for applications with higher energy storage requirements and where cost is a driving factor. There are salient operating characteristics of these devices that directly pertain and influence system design.

A. Battery Operation

Batteries are perhaps an obvious choice for this application due to the low power levels and requirement for long unattended, maintenance-free life. Long system life may be achieved with batteries, by using the battery manufacturer's reported performance and lifetime derating as it ages as a design consideration when designing the battery pack, similar to what has recently been done for batteries in other commercial products. According to industry standards, batteries designed for deep cycling are usually rated for 500 cycles at 80% depth-of-discharge (DOD), or about 1.4 years of daily cycling [25]. Engineers who design with batteries know that the DOD has a significant effect on the cycle life of lead–acid batteries [26]–[28]. Battery users appreciate that rated lifetimes are often not achieved in practice, particularly in demanding applications such as hybrid-electric vehicles [29]–[32], because the DOD, charging regime, and battery temperature strongly influence the expected lifetime [26], [27], [33], [34]. More recently, hybrid vehicles using nickel–metal hydride (NiMH) batteries have incorporated state-of-charge (SOC) control to ensure that the batteries are never fully recharged [31], which helps achieve long lifetime in that application. The result is that after operating at 40 °C and a 1-h discharge rate for ten years, the capacity is estimated to decrease by only 20% [35]. Proper charge management is paramount to achieving long battery life in this application.

The temperature of the environment in which the system is deployed is an important battery selection consideration. In general, operation at higher temperatures will cause batteries to degrade faster and temperatures that are too cold will limit or restrict charge and discharge processes. There are a wide variety of batteries, and each has its own charge and discharge operating temperature range that must be considered.

B. Battery Technologies

Lead–acid batteries are low-cost and are available in flooded or sealed designs. With flooded cells, the electrolyte is open to the atmosphere, so the batteries require frequent watering to replace evaporation losses. The maintenance requirements and hazard of exposed acid preclude flooded lead–acid batteries in this application. Lead–acid batteries are also available as sealed, "maintenance-free" designs such as the valve-regulated lead–acid (VRLA) battery. This design eliminates the spill hazard and watering requirement. Since VRLA are sealed batteries, overcharge equalization cannot be performed and active equalization may be necessary to maximize lifetime [36]. A concern with VRLA technology is thermal runaway during charging, which must be prevented. In general, temperature reduces the expected lifetime of lead–acid batteries by a factor of 2 for every 8 °C above 25 °C. In addition, to get the longest cycle lifetime, the battery should be designed to use only the first 20% SOC. Lead-based batteries also present a significant end-of-life disposal challenge. Thus, neither of these two common types of lead–acid batteries is suitable for unattended, long-term, daily cycling applications.

Nickel–cadmium (NiCd) batteries have many advantages over lead–acid batteries including long life and extended operating temperature range, and are thus a good candidate for battery technology. However, a significant disadvantage is the well-known environmental impact of the cadmium material that would require special end-of-life handling and recycling. Additionally, the so-called memory effect requires special charge management considerations such as periodic complete discharges that would limit the availability of the energy system [33].

NiMH cells share many of the same characteristics as NiCd batteries and mitigate many of the disadvantages. The most obvious improvement is the reduced environmental impact. They also have higher specific energy and energy density that makes them attractive for demanding applications such as hybrid vehicles [31]. However, they are less tolerant to overcharging than NiCd and lead–acid cells, necessitating good charge-management control. Charge management is particularly challenging in a solar-based system [37]. In some situations with limited temperature ranges, these batteries may be good candidates.

Lithium-ion batteries are the most recent cell technology, and there are many newer varieties of these cells that may be applicable for the present application. Lithium-ion cells are often specified for use in high-performance applications where size and performance are of paramount importance. They have a higher specific energy and energy density than NiMH cells but must be properly managed to avoid safety risks. Newer technologies that use polymer electrolytes or nanoscale lithium-iron phosphate cathodes are much more stable than older cobalt chemistries, so they yield extended cycle lifetimes and a wider temperature range.

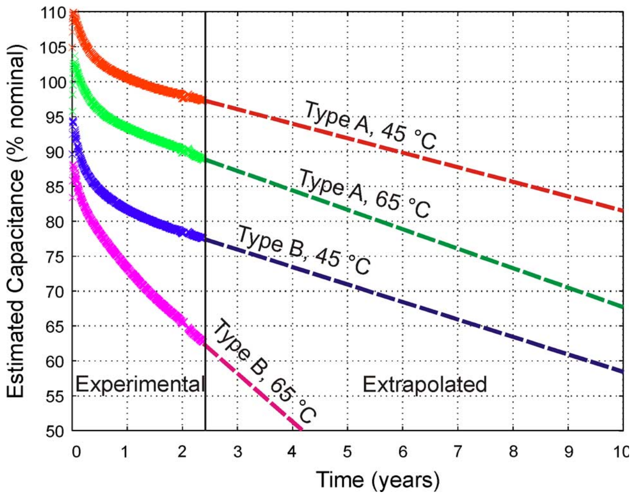

Fig. 9. Experimental and extrapolated capacity of ultracapacitors under daily cycling at elevated temperature.

C. Ultracapacitors

Ultracapacitors have dramatically different characteristics than batteries or standard capacitors. The double-layer effect near the surface of the electrode allows extremely high capacitance, albeit with a limited operating voltage of about 2.7 V [38]. Typical ultracapacitor applications tend to exploit their high power density; however, ultracapacitors are of interest here because their energy density is higher than conventional electrolytic capacitors. Ultracapacitors also offer much greater operational lifetime than batteries in extreme climates, a key feature in locations where maintenance is impossible, expensive, or inconvenient.

Testing over a 2.4-year period shows that ultracapacitors can have very long lifetimes with minimal capacity degradation. Fig. 9 shows the residual capacity of several ultracapacitors (relative to their nominal rated value) under a daily cycling application. It is seen that the performance of an ultracapacitor depends upon the temperature at which it is operated and that there are significant variations between manufacturers. Consistency within a single manufacturer was very good. Only ultracapacitors from manufacturer "A" are considered due to their superior lifetime performance. The results indicate that after four years of daily cycling, these ultracapacitors will retain over 80% of their initial capacity when held at a constant temperature of 65 °C. After ten years at this temperature, they are expected to retain over 65% of their initial capacity. If the temperature is less than 65 °C, the residual capacitance will be even higher. A system designed with ultracapacitors is sized such that at the end of life, it still has adequate energy storage capability to meet the availability requirements.

V. Maximum Power Point Tracking

System performance is substantially increased if maximum electrical power is available from the solar panel at all times given the available insolation. Many MPPT methods have been suggested over the past few decades; the relative merits of the most common method are discussed in [21]. In a long-term remote power supply, the need for high availability implies the need to harness maximum energy. This is particularly critical during days with low insolation. In full sun conditions, any significant fraction of the available solar electrical power will recharge the system quickly—MPPT simply affects how quickly the energy storage is replenished. However, maximizing the available solar electric power during low insolation periods can substantially alter system performance. The single worst day for Seattle in the 30-year dataset provided a total of 156 Wh/m^2 of energy. During this day, the *peak* hour of insolation provided only 44 W/m^2 (4.4% of full sunlight). An MPPT controller and converter optimized for low insolation will significantly reduce the energy storage requirement.

The controller must be designed for low power consumption, which translates into low complexity. Digital methods are strongly preferred due to the proliferation of low-power microcontrollers and programmable logic devices. Considering the MPPT techniques listed in [21], candidate techniques include perturb-and-observe (P & O), fractional open-circuit voltage ($V_{\rm oc}$), and best fixed voltage (BFV). Ripple correlation control (RCC) has low complexity, but is an analog method. An alternative, which was published after [21], is discrete-time RCC (DRCC), which translates RCC into a digital framework [16], [39]. Each approach has certain advantages and disadvantages for the present application. P & O and DRCC are both more accurate than the others, but require current sensors. The choice ultimately depends on the power consumption and accuracy of the specific implementation. The prototypes discussed in Section VIII used either fractional $V_{\rm oc}$ (for the smaller units) or DRCC.

The power converter must also be optimized for light-load efficiency. Although this may cause full-load efficiency to suffer, energy is abundant when the converter is at full load; so losses can be tolerated. This design philosophy is the exact opposite of the principles applied to an on-grid system design, where maximum energy production is desired at all times.

VI. Modularity and Expandability

A modular approach to power supply design can broaden the applicability of a particular design. Consider a unit rated to deliver 5 Wh per day in a given location; then a new application arises that requires up to 10 Wh per day. One option is to design a new system with a larger PV panel, more energy storage, and power converters optimized for this new power level. This design approach implies a high degree of customization based on location, desired availability, and load profile. Another option is to have designed the controller in the original unit such that two 5 Wh per day units can be connected in parallel to deliver the required 10 Wh per day. Extending this concept, an arbitrary number of identical units can be configured to support any number of applications including different geographic locations, load profiles, and availability requirements. This modular approach reduces time to market, increases economies of scale, and lowers overhead by stocking one model.

In order to support a modular architecture, each unit's controller must manage two objectives: MPPT for each unit must operate independently to harness maximum combined system power and the ESI must manage local energy storage in a system-coordinated way. This means that if any of the energy storage devices in a multiunit system can accept more energy, all of the MPPT converters should be active. If all energy storage devices are operated at nearly the same SOC, all ESI converters turn on and off together. Proper coordination of the ESI converters is needed to minimize circulation of power between the units that can excite intermodule oscillations and cause nuisance tripping of overload sensing and other protection functions [40].

There are many control architectures that can support modularity including a centralized controller, peer-to-peer agents, and distributed local controls [41]. A centralized controller can be highly effective, but adds cost and the potential for a single-point failure. Peer-to-peer communications nearly achieve the same level of performance as a centralized controller without the possibility of a single-point failure. However, if the communications link is disrupted, the system may again fail. Distributed local controls add some complexity to each module to provide the highest level of fault tolerance. The designer must trade fault tolerance against complexity and power consumption when choosing the system architecture.

VII. Fault Protection

A remote system must continue to operate in the event of foreseeable faults. The power circuit should be designed so that the system will continue to operate in the event of one or more component failures. Additionally, control circuitry should ensure that internal or external faults cause only transient disruption. Recall that the power source cannot be repaired. Instead, it must self-recover from all faults. Thus, concepts like mean time to repair (MTTR) are irrelevant here. Otherwise, the fault-tolerant concepts previously discussed for telecommunications power systems are appropriate [42], [43].

The topology in Fig. 1 has certain advantages when considering internal or external faults. The MPPT converter is shown as a boost converter. If the MOSFET fails to open, or the corresponding gate driver fails, the solar panel will still provide some power through the diode. If there is an external fault, the ESI converter can be temporarily disabled until the fault clears, then automatically brought back online. Other control circuitry can protect the system through black start and other unusual operating modes.

Additional fault tolerance is achieved through a modular design that can be implemented in an " N+1" system configuration [44]. As noted in Section III, the availability varies with the amount of energy storage and generation available. If a modular system loses one module while the others continue to function, the availability will degrade. However, the system will still have much greater availability than a single power source that fails.

If extreme fault tolerance is required, the controller can also be designed with internal redundancy, as in [45]. In most cases, the controller is the least likely item to fail in the power converter, so this extra level of redundancy is not necessary.

VIII. Experimental Results

A number of demonstration units, some of which are shown in Fig. 10, were built to validate the design methodologies presented in this paper. All of these ForeverPower units share certain features, as indicated in Fig. 1. The MPPT converters are boost converters; some were controlled with a fractional $V_{\rm oc}$ method, while others used DRCC. The ESI converters are bidirectional boost converters with sensorless current mode control [46]. The controllers have several operating modes for charge management and fault protection, and support modularity for increased power and energy capability. Various battery technologies and ultracapacitor combinations have been tested. Most units use multicrystalline silicon PV panels.

Fig. 10. Demonstration units with a variety of solar panel and energy storage configurations, deployed for testing in Champaign, IL.

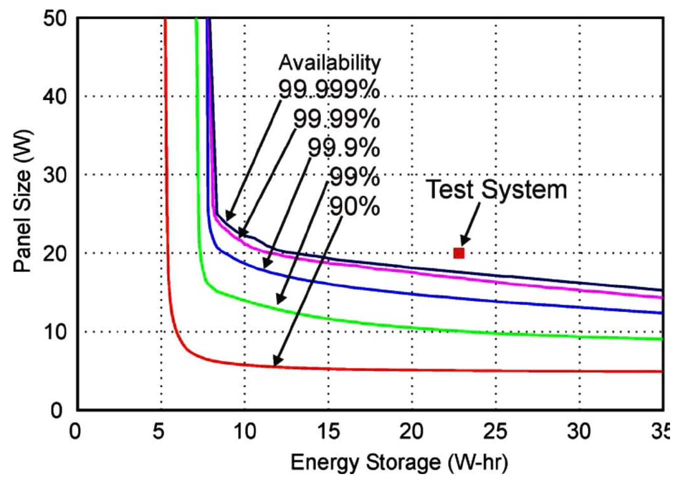

Fig. 11. Test system location on availability of Pareto chart for Champaign, IL.

In all cases, the design followed the principles of Fig. 2. Some of the devices were designed for other locations, but most were designed for Champaign, IL. Availability was always chosen as 100%, and the design lifetime varied from four to ten years. For cost reasons, multicrystalline silicon panels were used, but advanced triple junction cells were also considered where size was a critical factor. The selection of batteries or ultracapacitors depended on overall size restrictions.

One particular unit, which used a 22.8-Wh lithium–iron–phosphate battery for energy storage and a 20-W multicrystalline silicon PV panel, is indicated on the sizing chart of Fig. 11 for a daily load of 11.9 Wh. Time-domain results are shown in Fig. 12 . Positive PV panel voltage indicates when the sun was shining, which also correlates to an increase in panel temperature due to solar heating. Positive battery current recharges the battery and

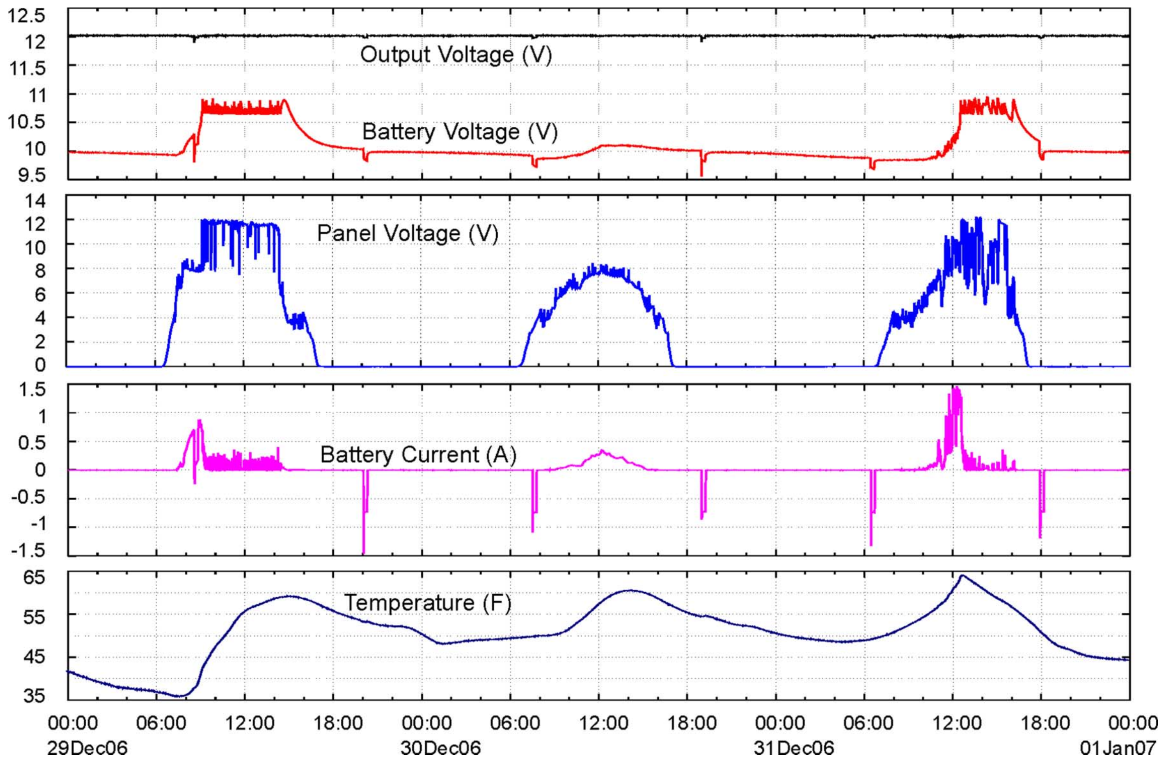

Fig. 12. Data from deployed demonstration unit in Champaign, IL.

negative current discharges to supply the load. The system was set to regulate the output to 12 V and was able to maintain this output level for the duration of the extended test.

The first day (December 29, 2006) was a relatively sunny day and the unit became fully charged, as indicated by the battery voltage going above 10.5 V. A hysteretic charge controller was used to approximate a "float" charge and maintain battery voltage as long as solar energy was available. The next day was overcast, so the unit did not get fully charged and had to draw more energy from the battery than on the first day. The third day again had enough incident solar energy to fully charge the battery. Thus, the battery acts as a buffer to meet the system load when there is not enough incident solar energy. The load consisted of a 312-mW base load (7.5 Wh per day) with a pulsed load that fired every 11 h. During each pulse, approximately 2 Wh of energy is extracted from the battery. These pulses can be seen on the battery current trace in the figure. Overall, approximately 11.9 Wh of energy is provided to the load each day from the system.

The challenges in the summer are different. In general, a system sized for high availability during the cloudiest portions of the year will have adequate energy generation during the sunny portions of the year, i.e., almost all summer days resemble the first day shown in Fig. 12, where the battery quickly reaches full charge. However, the enclosure must be designed to minimize the temperature of the energy storage devices. Higher operating temperature reduces operating lifetime. The thermal design of the system is beyond the scope of this paper, but is an important consideration for a practical device.

IX. Conclusion

This paper presented a new design approach for a power source for remote, unattended loads, such as sensors. The new system, which harvests solar energy and stores it in lithium-type batteries or ultracapacitors, is appropriate for applications that require more energy than can be provided with primary batteries. An important contribution was a sizing program that considers climatic data, energy storage capacity, energy generation capacity, and system efficiency. For a desired level of availability, there is a Pareto curve that relates energy storage to energy generation. The designer may choose a point on the curve that satisfies cost, size, or other requirements. The sizing was based on watt-hours and watts, which can then be translated into solar panel area and energy storage device volume. The system will then be optimally sized, rather than being oversized for worst-case scenarios.

An exemplary system topology was also shown. This topology achieves all of the goals of a remote power source: fault-tolerance, energy flow management, MPPT, and modularity. Several prototypes have been constructed. A representative three-day period was shown for a prototype that used multicrystalline silicon cells and lithium–iron–phosphate batteries. The results confirm that the system is capable of providing continuous power to a time-varying load.

References

[1] "National Renewable Energy Laboratory (NREL). (2008, Oct. 9).," in National Solar Radiation Data Base (NSRDB) 1961–1990 2008 [Online]. Available: http:// rredc.nrel.gov/solar/old_data/nsrdb/ 1961–1990/, [Online]. Available:

[2] R. N. Torah, M. J. Tudor, K. Patel, I. N. Garcia, and S. P. Beeby, "Autonomous low power microsystem powered by vibration energy harvesting," in *Proc. IEEE Sens. Conf.*, Oct. 28-31, 2007, pp. 264–267.

[3] P. D. Mitcheson , T. C. Green, E. M. Yeatman, and A. S. Holmes , "Architectures for vibration-driven micropower generators ," *J. Microelectromech. Syst.*, vol. 13, pp. 429 –440, Jun. 2004.

[4] S. Meninger, J. O. Mur-Miranda, R. Amirtharajah, A. P. Chandrakasan , and J. H. Lang, "Vibration-to-electric energy conversion," *IEEE Trans. Very Large Scale Integr. (VLSI) Syst.*, vol. 9, no. 1, pp. 64– 76, Feb. 2001.

[5] T.-K. Chung, D.-G. Lee, M. Ujihara, and G. P. Carman, "Design, simulation, and fabrication of a novel vibration-based magnetic energy harvesting device," in *Proc. Int. Solid-State Sens., Actuators Microsyst. Conf.* , Jun. 10–14, 2007, pp. 867 –870.

[6] T. S. Paing and R. A. Zane, "Resistor emulation approach to low-power energy harvesting," in *Proc. IEEE Power Electron. Spec. Conf.*, Jun. 18–22, 2006, pp. 1–7.

[7] T. Le, K. Mayaram, and T. Fiez, "Efficient far-field radio frequency energy harvesting for passively powered sensor networks," *IEEE J. Solid-State Circuits* , vol. 43, no. 5, pp. 1287–1302, May 2008.

[8] M. A. Weimer, T. S. Paing, and R. A. Zane, "Remote area wind energy harvesting for low-power autonomous sensors," in *Proc. IEEE Power Electron. Spec. Conf.*, Jun. 18--22, 2006, pp. 1–5.

[9] Y. K. Tan and S. K. Panda, "A novel piezoelectric based wind energy harvester for low-power autonomous wind speed sensor ," in *Proc. 33rd Annu. Conf. IEEE Ind. Electron. Soc.*, Nov. 5–8, 2007, pp. 2175–2180.

[10] C. Park and P. H. Chou, "AmbiMax: Autonomous energy harvesting platform for multi-supply wireless sensor nodes ," in *Proc. IEEE Commun. Soc. Conf. Sens. Ad Hoc Commun. Netw.*, Sep. 28, 2006, vol. 1, pp. 168–177 .

[11] R. Myers, M. Vickers, H. Kim, and S. Priya, "Small scale windmill," *Appl. Phys. Lett.*, vol. 90, pp. 054106-1–054106-3, Jan. 2007.

[12] B. T. Kuhn and R. S. Balog, "Design considerations for long-term remote photovoltaic-based power supply," in *Proc. IEEE Appl. Power Electron. Conf.,*, Feb. 24–28, 2008, pp. 154–159.

[13] V. Raghunathan, A. Kansal, J. Hsu, J. Friedman, and M. Srivastava, "Design considerations for solar energy harvesting wireless embedded systems," in *Proc. 4th Int. Symp. Inf. Process. Sens. Netw.*, Apr. 15, 2005, pp. 457–462.

[14] F. I. Simjee and P. H. Chou, "Efficient charging of supercapacitors for extended lifetime of wireless sensor nodes ," *IEEE Trans. Power Electron.*, vol. 23, no. 3, pp. 1526–1536, May 2008.

[15] J. W. Kimball, P. T. Krein, and N. D. Benavides, "Modular system for unattended energy generation and storage," U.S. Patent application 11/615,074 submitted , Dec. 2006.

[16] J. W. Kimball and P. T. Krein, "Ripple correlation control based on limited sampling," U.S. Patent application 11/626,911, submitted, Jan. 25, 2007.

[17] J. W. Kimball, P. T. Krein, and N. D. Benavides, "Apparatus and method for controlling a power supply," U.S. Patent application 11/627,731, submitted , Jan. 26, 2007.

[18] H. Al-Atrash, F. Tian, and I. Batarseh, "Tri-modal half-bridge converter topology for three-port interface," *IEEE Trans. Power Electron.*, vol. 22 , no. 1, pp. 341–345, Jan. 2007.

[19] M. Marchesoni and C. Vacca, " New dc–dc converter for energy storage system interfacing in fuel cell hybrid electric vehicles," *IEEE Trans. Power Electron.*, vol. 23, no. 1, pp. 107–115, Jan. 2008.

[20] D. Liu and H. Li, "A ZVS bi-directional dc–dc converter for multiple energy storage elements," *IEEE Trans. Power Electron.*, vol. 21, no. 5, pp. 1513–1517, Sep. 2006.

[21] T. Esram and P. L. Chapman, "Comparison of photovoltaic array maximum power point tracking techniques," *IEEE Trans. Energy Convers.*, vol. 22, no. 2, pp. 439–449, Jun. 2007.

[22] M. Stan, D. Aiken, B. Clevenger, A. Cornfeld, J. Doman, E. Downard, J. Hills, R. Hoffman, G. Johnston, F. Newman, J. Pappan, A. Sandoval , P. Sharps, and J. Wood, "Design and performance of high efficiency III–V space solar cells with monolithic bypass diode architecture," in *Proc. IEEE World Conf. Photovoltaic Energy Convers.*, May. 2006, vol. 2, pp. 1865–1868.

[23] *Standard Tables for Reference Solar Spectral Irradiances: Direct Normal and Hemispherical on 37° Tilted Surface* , ASTM International Standard G173, 2003.

[24] P. F. Ribeiro, B. K. Johnson, M. L. Crow, A. Arsoy, and Y. Liu, "Energy storage systems for advanced power applications," *Proc. IEEE*, vol. 89, no. 12, pp. 1744–1756, Dec. 2001.

[25] *Secondary Cells and Batteries Containing Alkaline or Other Non-Acid Electrolytes—Portable Sealed Rechargeable Single Cells—Part 2: Nickel-Metal Hydride (Supersedes IEC 61436)*, International Electrotechnical Commission (IEC) Standard 61951-2, 2003.

[26] D. G. Vutetakis and H. Wu, "The effect of charge rate and depth of discharge on the cycle life of sealed lead–acid aircraft batteries ," in *Proc. Power Sources Symp.*, 1992, pp. 103–105.

[27] L. H. Thaller, "Expected cycle life vs. depth of discharge relationships of well-behaved single cells and cell strings," *J. Electrochem. Soc.*, vol. 130, pp. 986–990, May 1983.

[28] P. J. Johnson and P. E. Miles, "In-orbit performance of batteries on the Skynet 4 spacecraft fleet: A nickel-cadmium success story ," in *Proc. NASA Aerosp. Battery Workshop*, 1996, pp. 451–467.

[29] W. Jong-Seob, R. Langari, and M. Ehsani, "An energy management and charge sustaining strategy for a parallel hybrid vehicle with CVT," *IEEE Trans. Control Syst. Technol.*, vol. 13, no. 2, pp. 313–320 , Mar. 2005.

[30] B. E. Dickinson and D. H. Swan, "EV battery pack life: Pack degradation and solutions," in *Proc. Future Transp. Technol. Conf. Expo.*, 1995, pp. 145– 154, Tech. Rep. 951949.

[31] K. J. Kelly, M. Mihalic, and M. Zolot, "Battery usage and thermal performance of the Toyota Prius and Honda Insight during chassis dynamometer testing," in *Proc. Battery Conf. Appl. Adv.*, 2002, pp. 247–252.

[32] L. Chan-Chiao, K. Jun-Mo, J. W. Grizzle, and P. Huei, "Energy management strategy for a parallel hybrid electric truck," in *Proc. Amer. Control Conf.*, 2001, vol. 4, pp. 2878–2883.

[33] D. Linden and T. B. Reddy*, Handbook of Batteries*, 3rd ed. New York: McGraw-Hill , 2002.

[34] D. Walthew, "A novel approach to managing battery capacity and lifecycle–-Based on: Climate, environment and usage type," in *Proc. Int. Telecommun. Energy Conf. (INTELEC)* , 2003, pp. 671–678.

[35] R. S. Balog, "Fig1. The estimate of 1lt discharge voltage curve (HHR650D) after 10 years of intermittent charge life at 25 deg C," in Aug. 21, 2006 , Panasonic, private communication.

[36] P. T. Krein and R. S. Balog, "Life extension through charge equalization of lead–acid batteries," in *Proc. Int. Telecommun. Energy Conf. (INTELEC)*, 2002, pp. 516–523.

[37] F. Boico, B. Lehman, and K. Shujaee, "Solar battery chargers for NiMH batteries," *IEEE Trans. Power Electron.*, vol. 22, no. 5 , pp. 1600–1609, Sep. 2007 .

[38] G. L. Bullard, H. B. Sierra-Alcazar, H. L. Lee, and J. L. Morris, "Operating principles of the ultracapacitor," *IEEE Trans. Magn.*, vol. 25, no. 1, pp. 102 –106, Jan. 1989.

[39] J. W. Kimball and P. T. Krein, "Digital ripple correlation control for photovoltaic applications," in *Proc. IEEE Power Electron. Spec. Conf.*, Jun. 17-21, 2007, pp. 1690–1694.

[40] R. S. Balog and P. T. Krein, "Bus selection in multibus DC power systems," in *Proc. Electr. Ship Technol. Symp. (ESTS)*, May. 21–23, 2007, pp. 281–287.

[41] R. S. Balog, "Autonomous local control in distributed DC power systems,," Ph.D. dissertation, Univ. Illinois, Urbana-Champaign, 2006.

[42] R. V. White and F. M. Miles, "Principles of fault tolerance," in *Proc. Appl. Power Electron. Conf.* , 1996, vol. 1, pp. 18–25.

[43] R. V. White, "Using redundant dc power in high availability systems," in *Proc. Appl. Power Electron. Conf.*, 2006, pp. 848 –853.

[44] F. Shi, A. Sullivan, and H. Sahagian, "Integrated power systems with fault tolerant attributes," in *Proc. Appl. Power Electron. Conf.*, 1997 , vol. 1, pp. 443–447.

[45] K. Shimamura, Y. Morita, Y. Takahashi, T. Hotta, S. Ueda, M. Nohara, M. Kido, S. Tanaka, K. Imaie , K. Sakamoto, and T. Nakajima, "A triple redundant controller which adopts the time-sharing fault recovery method and its application to a power converter controller ," in *Proc. IEEE Real-Time Technol. Appl. Symp.*, Jun. 3-5, 1998, pp. 210–219.

[46] P. Midya, P. T. Krein, and M. F. Greuel, "Sensorless current mode control—An observer-based technique for dc–dc converters," *IEEE Trans. Power Electron.*, vol. 16, no. 4, pp. 522–526 , Jul. 2001.

Jonathan W. Kimball (S'96–M'96–SM'05) received the B.S. degree in electrical and computer engineering from Carnegie Mellon University, Pittsburgh, PA, in 1994, the M.S. degree in electrical engineering and the Ph.D. degree in electrical and computer engineering from the University of Illinois, Urbana-Champaign, in 1996 and 2007, respectively.

From 1996 to 1998, he was with Motorola, Phoenix, AZ, where he designed insulated gate bipolar transistor (IGBT) modules for industrial applications. He then joined Baldor Electric, Fort Smith, AR, where he designed industrial adjustable-speed drives ranging 1–150

hp. In 2003, he returned to Illinois as a Research Engineer (later a Senior Research Engineer). Later in 2003, he cofounded SmartSpark Energy Systems, Inc., Champaign, IL, where he was the Vice President of Engineering. In 2008, he joined Missouri University of Science and Technology (Missouri S&T), Rolla, where he is currently an Assistant Professor.

Dr. Kimball is a member of Eta Kappa Nu, Tau Beta Pi, and Phi Kappa Phi. He is also a Licensed Professional Engineer in the State of Illinois.

Brian T. Kuhn (S'94–M'97–SM'07) received the B.S. and M.S. degrees in electrical engineering from the University of Missouri, Rolla, in 1996 and 1997, respectively.

He was a Research Engineer at Purdue University for six years, and investigated power-electronics-based systems, where he also took seven graduate-level courses. Specifically, he designed and implemented many power converter circuits at power levels up to 75 kW. Since 2004, he has been with SmartSpark Energy Systems, Inc., where he is involved in the design and development of the BattEQ line of battery equalizers and the ForeverPower remote unattended power supplies. His current research interests include the development of the SolarBridge line of inverters.

Mr. Kuhn is a member of Eta Kappa Nu and Tau Beta Pi.

Robert S. Balog (S'92–M'96–SM'07) received the B.S. degree in electrical engineering from Rutgers – The State University of New Jersey, New Brunswick, and the M.S. and Ph.D. degrees in electrical engineering from the University of Illinois at Urbana-Champaign, Urbana.

From 1996 to 1999, he was an Engineer at Lutron Electronics, Coopersburg, PA. From 1999 to 2006, he was a Research and Teaching Assistant in the Power Electronics Laboratory, University of Illinois. Since 2006, he has been a Senior Engineer at SmartSpark Energy Systems, Inc., Champaign, IL. He holds two issued U.S. patent with additional U.S. and foreign patents pending. He is also the author or coauthor of 16 published papers. His current research interests include power converters for solar energy, particularly microinverters for ac photovoltaic (ACPV) modules.

Dr. Balog is a Registered Professional Engineer in Illinois. He was the first Fellow of the International Telecommunications Energy Conference. He is a member of Eta Kappa Nu, the Electric Manufacturing and Coil Winding Association, the Illinois Society of Professional Engineers, and the National Society of Professional Engineers.